Journal of Medicinal Chemistry Article

J. Med. Chem. **2010,** *53,* 7129–7139 **7129**
DOI: 10.1021/jm100832d

Exploration of the Amine Terminus in a Novel Series of 1,2,4-Triazolo-3-yl-azabicyclo[3.1.0]hexanes as Selective Dopamine D_3 Receptor Antagonists

Fabrizio Micheli,*[,§,†] Luca Arista,[#] Barbara Bertani,[§,†] Simone Braggio,[§,†] Anna Maria Capelli,[§,‡] Susanna Cremonesi,[§,†] Romano Di-Fabio,[§,†] Giacomo Gelardi,[§,†] Gabriella Gentile,[§,†] Carla Marchioro,[§,‡] Alessandra Pasquarello,[§,†] Stefano Provera,[§,‡] Giovanna Tedesco,[§,‡] Luca Tarsi,[§,†] Silvia Terreni,[§,†] Angela Worby,[∥,‡] and Christian Heidbreder[⊥]

[†]*Neurosciences Centre of Excellence, and* [‡]*Molecular Discovery Research,* [§]*GlaxoSmithKline Medicines Research Centre, Via Fleming 4, 37135 Verona, Italy,* [∥]*NFSP, Harlow, U.K.,* [⊥]*Reckitt Benckiser Pharmaceuticals, Richmond, Virginia 23235, and* [#]*Novartis Institute Research, Basel, Switzerland*

Received July 5, 2010

A novel series of 1,2,4-triazol-3-yl-azabicyclo[3.1.0]hexanes with high affinity and selectivity for the DA D_3 receptor and excellent pharmacokinetic profiles was recently reported. We also recently discussed the role of the linker associated with the triazole moiety. In this manuscript, we are reporting a detailed exploration of the region of the receptor interacting with the amine terminus of the scaffold wherein SAR and developability data associated with these novel templates was undertaken.

Introduction

Growing evidence arising from preclinical models of substance dependence suggests that selective DA D_3 receptor antagonists might be a potential approach for the pharmacotherapeutic management of substance dependence and addiction.[1−6] The data collected thus far suggest that selective DA D_3 receptor antagonists are efficacious in disrupting drug-associated cue-induced craving, hence preventing reinstatement of drug-seeking behavior. These findings have greatly contributed to the interest of medicinal chemists in developing new and highly selective ligands.

We have recently reported[7] a new series of 1,2,4-triazol-3-yl- azabicyclo[3.1.0]hexanes endowed with high affinity and selectivity at the DA D_3 receptor (**1**, Figure 1). These compounds have an excellent pharmacokinetic (PK[a]) profile and show efficacy in animal models of drug dependence. We have also recently explored[8] the role of the thiotriazole system by modifying the linker (**2**, Figure 1) and replacing the sulfur atom with oxygen and carbon. Also in this case, compounds endowed with good potency and a favorable PK profile were identified. In this rigorous exploration of selective DA D_3 receptor antagonists, the next logical step was to analyze the amine portion of the molecule. Considering that a benzazepine (BAZ) template[9] (**3**, Figure 1) and fused BAZ scaffolds[10,11] (**4**, **5**, Figure 1) were available in our collection and that selective compounds were also reported by others,[5] the in-house available pharmacophore model (Figure 2) mainly based on the structures of **SB-277011**[12] (Figure 1) and **SB-414796**[13] (Figure 1) was refined.[14] A schematic representation of this refined version is reported in Figure 3A with all the compounds reported in Figure 1 fitted in the model; Figure 3B represents only the 1,2,4-triazol-3-yl- azabicyclo[3.1.0]hexane scaffold (**1**). Further details on the model construction are available in the Supporting Information.

Despite the difficulty of understanding a three-dimensional arrangement that is plotted in a two-dimensional space, it is becoming evident that one of the hydrophobic regions was removed from the original model and that the aromatic region has now a slightly different positioning with respect to the positive ionizable region. Considering that the aim of the work was the identification of new amines that could potentially replace the azabicyclo[3.1.0]hexane system of scaffold **1**, it was important to focus the modeling work on this specific area. The first attempt was to design an "expanded" ring system with respect to the azabicyclo[3.1.0]hexane that could, however, maintain the same distance between the basic nitrogen and the centroid of the aromatic system. Accordingly, the regioisomeric 1-phenyl-3-azabicyclo[4.1.0]heptane (**6**, Figure 4A) and 6-phenyl-3-azabicyclo[4.1.0]heptane (**7**, Figure 4A) templates and the 1-phenyl-4-azabicyclo[5.1.0]octane (**8**, Figure 4A) scaffold were designed. Figure 4B shows an example of a single enantiomer of each of the fragments **6** and **7**. All these structures tend to fit quite well within these regions of the pharmacophore model in terms of key interaction points. Nonetheless, it is worth reporting that for all these new scaffolds, a portion of their structure cannot fully overlap (in terms of van der Waal's volumes) with the original smaller template; therefore, a potentially forbidden region might arise because of a steric clash within the active site of the receptor.

Results and Discussion

The synthesis of the final structures was performed through the alkylation of the desired 3-[(3-chloropropyl)thio]-4-methyl-5-aryl-1,2,4-triazole intermediate with the suitable amine,

*To whom correspondence should be addressed. Phone: +39-045-8218515. Fax: +39-045-8118196. E-mail: fabrizio.micheli@aptuit.com. Address: Aptuit Verona, Medicines Research Centre, Via Fleming 4, 37135 Verona, Italy.

[a] Abbreviations: hERG, human ether-a go-go related gene K^+ channel; NCE, new chemical entity; PK, pharmacokinetic; P450, cytochrome P450; hCli, human intrinsic clearance; *F*%, Bioavailability; B/B, brain/blood ratio; Clb, blood clearance; Vd, distribution volume; clogD, calculated logD; GPCR, G-protein coupled receptor; TM, trans membrane.

Published on Web 09/14/2010

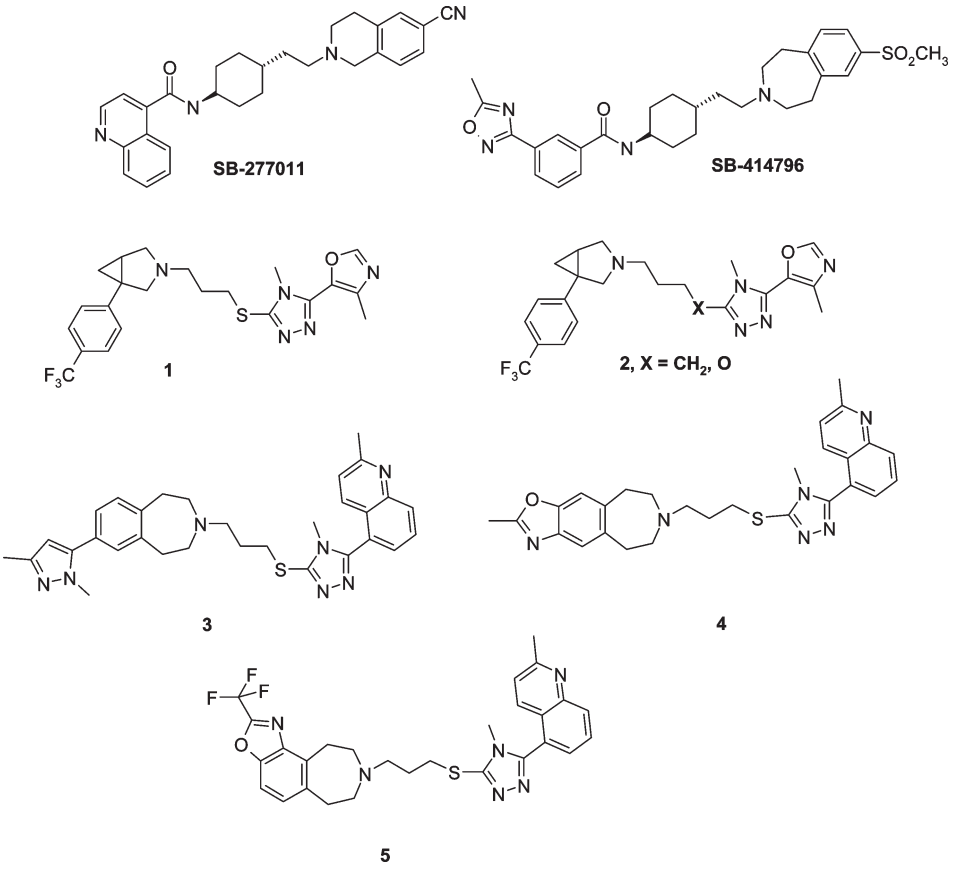

Figure 1. Structures of the previously reported GSK selective DA D_3 receptor antagonists.

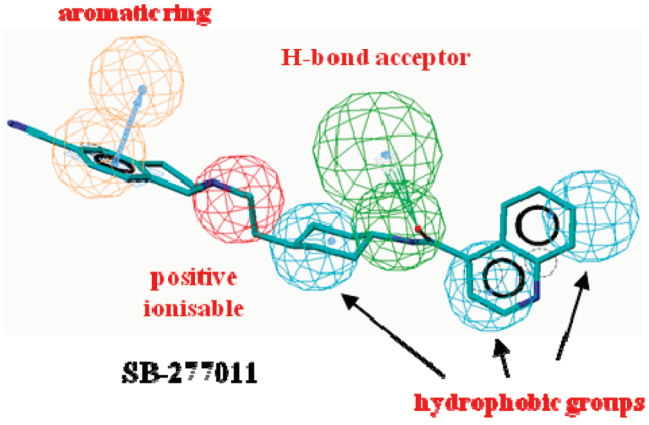

Figure 2. The original pharmacophore model derived from SB-277011 with the compound fitted. Red sphere, positive ionizable; cyan spheres, hydrophobic; green spheres, hydrogen bond acceptor; orange spheres, aromatic ring region.

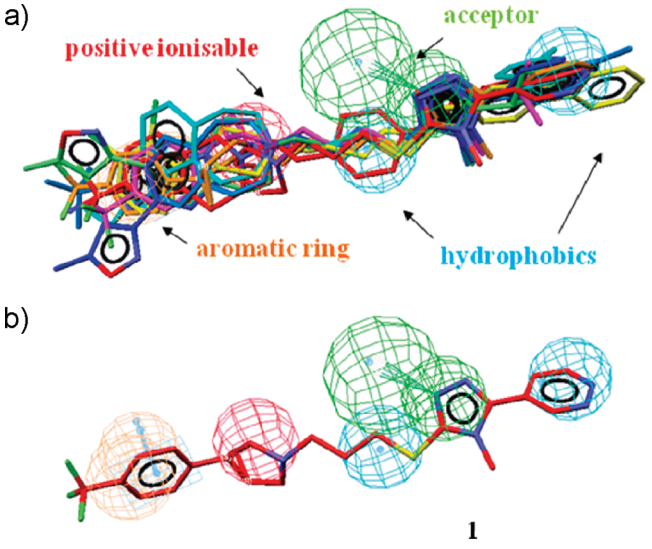

Figure 3. (A) The new pharmacophore model with some of the structures reported in Figure 1 fitted. Red sphere, positive ionizable; cyan spheres, hydrophobic; green spheres, hydrogen bond acceptor; orange spheres, aromatic ring region. (B) The new pharmacophore model with the [3.1.0] system fitted.

similarly to previously reported[7] reactions (a detailed synthetic scheme is available in the Experimental Section). The biological screening cascade for the progression of the new compounds is detailed elsewhere.[7] All the compounds were assayed for their agonist and antagonist properties using a functional GTPγS assay expressing the human DA D_3 receptor, the human DA D_2 receptor, and the human ether-a-go-go K^+ channel (hERG), a potential cardiovascular liability target (using the dofetilide binding assay). The results of this exploration are reported in Table 1.

When the racemic unsubstituted phenyl scaffolds were used (**9**, **10**), only poor activity was detected at the DA D_3 receptor. This was probably due to the low lipophilicity of these systems, similarly to some previously explored series.[7] The introduction of a 4-trifluoromethyl moiety on the phenyl group (**11**, **12**) achieved a more suitable ClogD profile with good potency and selectivity. Specifically, the 1-phenyl-3-azabicyclo[4.1.0]heptane **11** had higher DA D_3 receptor affinity compared to the regioisomeric 6-phenyl derivative **12**, leading

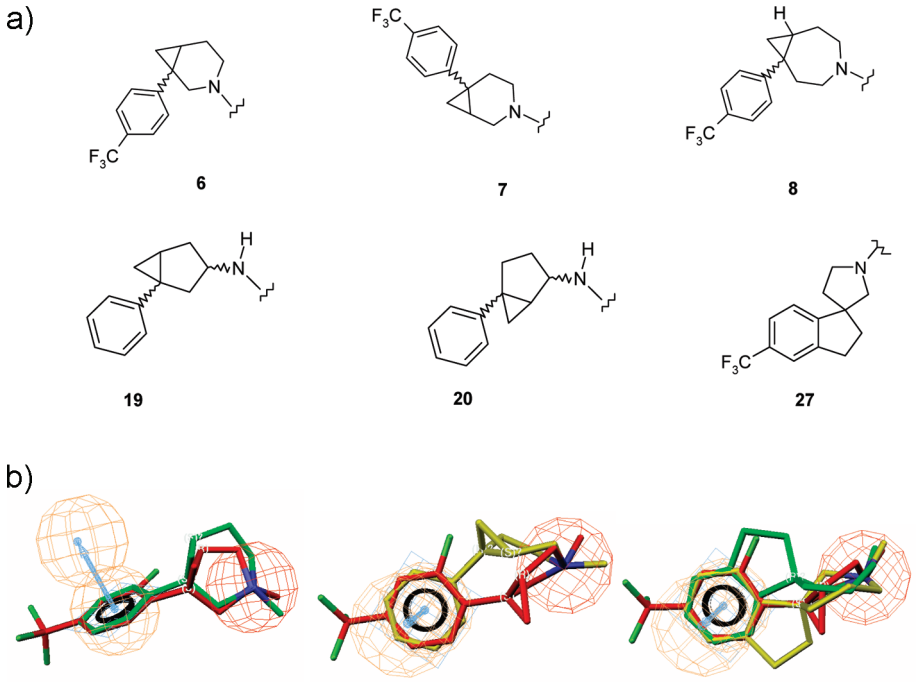

Figure 4. (A) A series of structures which may represent potential alternative to the azabicyle[3.1.0]hexane system. (B) The fitting in the pharmacophore model (only the positive ionizable and aromatic region are reported) of structure **6** (left panel, one enantiomer colored in green), structure **7** (middle panel, one enantiomer colored in gold), and structure **27** (right panel, two enantiomers colored in green and gold) with respect to the azabicyclo[3.1.0]hexane **1** (1*S*,5*R* enantiomer colored in red).

to a 60-fold selectivity vs the DA D_2 receptor. When the 3 positions of the phenyl group were explored, the 6-phenyl-3-azabicyclo[4.1.0]heptane **14** became now more potent and selective at the DA D_3 receptor compared to **13**; unfortunately, the activity of **14** at the hERG channel was also relatively high and the compound was not progressed. The increased bulkiness of the bicyclic ring moving to the 1-phenyl-4-azabicyclo[5.1.0]octane system was not detrimental to the DA D_3 affinity (**15**−**18**), but the selectivity at the DA D_2 receptor had to be fine-tuned. The slightly higher lipophilicity of derivatives (**15**−**17**) with respect to **1** was probably the cause of the increased affinity at the D_2 receptor. The careful design of the substituents used to decorate the right-hand-side of this new template proved that this scaffold was worth further investment. For example, the introduction of the pyridazine moiety (**18**) achieved the same ClogD as derivative **1** and led to a molecule endowed with a 100-fold selectivity over the D_2 receptor. As previously described,[7] each promising compound was profiled along the screening cascade to ensure appropriate PK and developability characteristics. When tested in the CYPEX bactosome P450 inhibition test and in the rat and human in vitro clearance (Cli) in liver microsomes, **18** showed a good profile: the IC_{50} values for all major P450 isoforms tested (CYP1A2, CYP2C9, CYP2C19, CYP2D6, and CYP3A4) were greater than 6 μM, and Cli values both in human and rat were moderately low (0.8 and 0.5 mL/min/g of protein, respectively).

Another approach aimed at maintaining a bicyclic system in the triazole scaffolds was the application of phenylbicyclo-[3.1.0]hexane amines as the source of basic moiety in the template. For this reason, the 1-phenylbicyclo[3.1.0]hexan-3-amine (**19**, Figure 4A) and the 5-phenylbicyclo[3.1.0]hexan-2-amine (**20**, Figure 4A) were selected despite a relatively low ClogD. Actually, for previously described templates,[7] a specific range of ClogD (between 2 and 4) was shown as optimal for maximizing the DA D_3 affinity. The results of the final compounds (**21**−**24**) are reported in Table 2. Despite the presence of a secondary amine, micromolar affinity was achieved at the DA D_3 receptor using amine **19**. Taking into consideration, however, the nonsubstituted nature of the phenyl group and the relatively high metabolic fate of derivative **21** (Cli = 2.6 and 5.4 mL/min/g of protein in human and rat, respectively), the research focused primarily on the 4-trifluoromethyl regioisomer **20**. Considering the presence of multiple stereocenters, the strategy was to proceed with a chiral separation of the four diastereoisomers; only three of the latter (**22**−**24**) showed appropriate purity characteristics for in vitro testing. Derivative **24**, one of the two enantiomers with a relative *trans* configuration between the secondary amine and the phenyl group, showed a low micromolar potency at the DA D_3 receptor and a 100-fold selectivity vs D_2 target. IC_{50} values for all P450 isoforms tested were greater than 4 μM and Cli values both in human and in rat were low (<0.5 mL/min/g of protein for both targets). Accordingly, this area was further developed and a fluorine atom was introduced to slightly increase the ClogD value. The effect of this substitution on the two reported *trans* derivatives (**25** and **26**) was greater on the less active enantiomer **26** at the DA D_3 receptor, leading to a more balanced profile. In contrast, compound **25** did not show any major improvement in desired affinity.

Another innovative template was then hypothesized to sit into the hydrophobic pocket close to the Asp110 region in the DA D_3 receptor.[15] From the docking studies performed in the receptor model and previously reported,[9−11] this region appeared relatively large because it was able to accommodate bulky substituents like the amine portion of the BAZ systems of derivatives **3**, **4**, **5**. Accordingly, a series of spiro derivatives

Table 1. Functional Activity at the Human DA D_3 Receptor and Selectivity for Derivatives **9**−**18**[a]

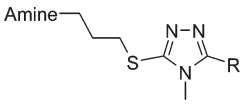

Entry*	Amine	R	hD_3-GTPγS fpKi	hD_{2L}-GTPγS fpKi	hERG pIC_{50}	cLogD[#]
1	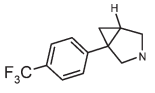		9.3	6.9	6.0	2.1
9	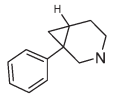		6.9	6.4	5.2	1.7
10	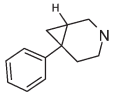		6.8	5.5	5.3	1.5
11	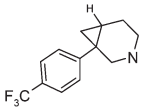		8.1	6.3	5.7	2.8
12	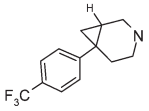		7.4	6.5	6.1	2.6
13	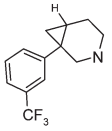		7.9	6.5	5.7	2.4
14	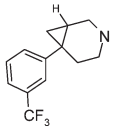		8.2	5.6	6.7	2.2
15	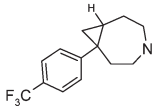		8.4	7.0	5.8	2.9
16	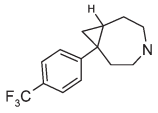	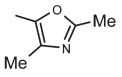	8.0	6.7	5.9	3.5
17	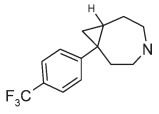	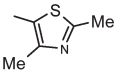	8.4	6.7	6.2	2.9
18	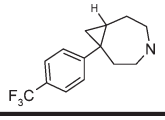		8.4	6.4	5.3	2.1

[a] fpK_i = functional pK_i obtained from the GTPγS functional assay. SEM for D_3 GTPγS, and HERG data sets is ±0.1 and for the D_{2L} GTPγS data is ±0.2. * All the compounds were tested as racemates. [#] ACD logD 7.4. Ver 11.

were designed and one of these scaffolds (**27**) is reported in Figure 4A. As it can be seen in the right panel of Figure 4B, both the enantiomers of this structure (the green and gold traces) fit well into the pharmacophore model when compared to the azabicyclo[3.1.0]hexane. From a theoretical standpoint, one of the two enantiomers (green) also seems to fit better in

Table 2. Functional Activity at the Human DA D_3 Receptor and Selectivity for 4 Derivatives **21**−**26**[a]

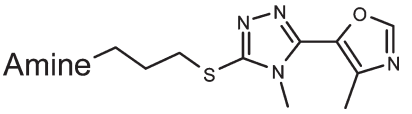

Entry*	Amine	hD_3-GTPγS fpKi	hD_{2L}-GTPγS fpKi	hERG pIC_{50}	cLogD[#]
21	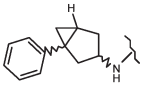	7.3	6.6	5.1	0.2
22 (s.e. 1)	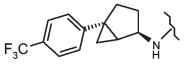	6.9	< 5.5	6.6	1.1
23 (s.e. 2)	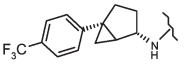	6.6	< 5.5	5.6	1.1
24 (s.e. 3)	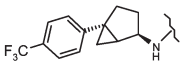	8.4	6.3	6.2	1.1
25 (s.e. 1)	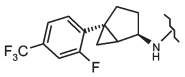	8.5	6.7	6.2	1.3
26 (s.e. 2)	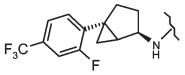	7.5	< 5.5	6.0	1.3

[a] fpK_i = functional pK_i obtained from the GTPγS functional assay. SEM for D_3 GTPγS, and HERG data sets is ±0.1; SEM for the D_{2L} GTPγS data is ±0.2. [#] ACD logD 7.4. Ver 11. * All the compounds were tested as racemates, unless specified (s.e. = single enantiomer). Relative stereochemistry is shown. Figures (1 to 3 for compounds **22**−**24**, and 1 to 2 for derivatives **25**−**26**) are added to identify the different single enantiomers.

terms of overlap of the van der Waal's volumes with the red structure; a series of derivatives were prepared and the biological results are reported in Table 3. The first part of the exploration was performed using a 3,4-dihydro-2*H*-spiro-[naphthalene-1,3′-pyrrolidine] system. Despite a relatively high ClogD, derivatives **28** and **29** were about 10-fold less potent at the DA D_3 receptor compared to **1**; the affinity at the DA D_2 receptor was similarly reduced while the hERG component remained unchanged. The reduction in lipophilicity caused by the introduction of a methoxy group further reduced the affinity at the desired target independent of its position on the aromatic ring (**30**−**32**), and this caused a decrease in the selectivity vs the DA D_2 receptor because the affinity at this target remained unchanged. The removal of the methoxy group and the introduction of the oxygen in the six-membered ring (**33**) had a positive impact on the reduction of the D_2 affinity. Improvement of desired activity at the D_3 receptor was obtained with the smaller 2,3-dihydrospiro-[indene-1,3′-pyrrolidine] template (**34**−**36**). The positioning of the bromine on the aromatic ring seemed to slightly increase the affinity at the primary target, but unfortunately this also went in the same direction for the secondary targets, thus limiting the selectivity of the scaffold to about 30-fold. The use of chlorine/fluorine together with a different heteroaromatic group in right-hand-side of the scaffold (**37**−**40**) did not modify the overall trend of this series. One may hypothesize that the steric bulk of these structures is relatively well tolerated by the DA D_3 receptor in terms of affinity, but it drastically changes the selectivity profile of this specific series, potentially distorting other key interactions within the DA receptors.

Finally, to conclude this part of the exploration, it was decided to probe the region with a series of 3-phenyl-8-azabicyclo[3.2.1]octanes. Table 4 reports some specific examples of this modification; more specifically, only the endo derivatives results are reported based on purity criteria. Derivative **41** showed nanomolar affinity at the DA D_3 receptor and a good in vitro PK profile was good despite the lipophilic nature of the *t*-Bu moiety on the aromatic ring. The IC_{50} values for all major P450 isoforms tested were greater than 5 μM and Cli values in humans were moderate (1.9 mL/min/g of protein); Cli values in rats were however high (7.9 mL/min/g of protein). Replacement with trifluoromethyl substituents (**42**) was performed to assess if Cli values were associated with the nature of the *t*-Bu group. In this derivative, the IC_{50} values for all P450 isoforms tested were greater than 10 μM and Cli values both in human and in rat were moderately low (0.9 and < 0.5 mL/min/g of protein, respectively). However, unexpected results were observed around the affinity profile: while a slight decrease in the DA D_3 affinity was expected, there was no similar decrease in DA D_2 affinity but a significant increase in the hERG affinity. It was postulated, therefore, that the decreased bulkiness of the CF_3- group allowed a different positioning of the phenyl group in the hERG channel, while the former substituent was bulky enough to prevent such interaction. To confirm this working hypothesis, docking experiments in the hERG channel model were performed in agreement with previously reported work.[7] A pictorial representation of the results is shown in Figure 5. In agreement with this model, the switch of the CF_3- group from the *para* to the *meta* position should disfavor such interactions. This was demonstrated by compound **43** with a 5-fold decrease in the hERG affinity. Unfortunately, in these specific derivatives, the decrease in hERG affinity was paralleled by a decreased affinity at both the D_2 and the D_3 receptors. To regain DA D_3 affinity in this particular subseries, the introduction of a fluorine atom in position *ortho* (**44**) fitted the purpose of changing both the

Table 3. Functional Activity at the Human DA D_3 Receptor and Selectivity for 5-Oxazolyl Derivatives **28**−**40**[a]

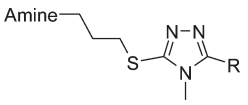

Entry*	Amine	R	hD_3-GTPγS fpKi	hD_{2L}-GTPγS fpKi	hERG pIC_{50}	cLogD[#]
28	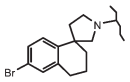		8.1	6.3	6.2	3.4
29	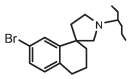		7.8	6.5	5.9	3.9
30	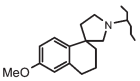		7.0	6.0	5.7	2.5
31	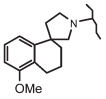		7.1	6.4	5.7	2.3
32	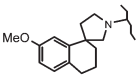		7.5	6.6	5.2	2.2
33	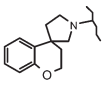		7.0	< 5.5	5.2	1.6
34	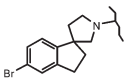		8.3	6.9	6.5	2.6
35	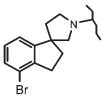		8.1	6.6	6.2	3.0
36	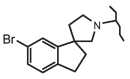		8.6	7.4	6.1	3.1
37	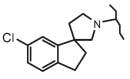	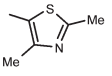	7.5	6.5	5.6	2.2
38	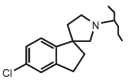	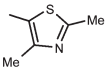	7.5	6.4	5.6	2.3
39	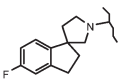	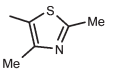	6.8	7.0	5.6	1.7
40	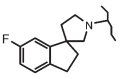	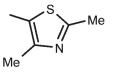	7.3	6.4	5.2	1.4

[a] fpK_i = functional pK_i obtained from the GTPγS functional assay. SEM for D_3 GTPγS, and HERG data sets is ±0.1; SEM for the D_{2L} GTPγS data is ±0.2. [#] ACD logD 7.4. Ver 11. * All the compounds were tested as racemates.

stereoelectronic nature of the aromatic ring and its position with respect to the tropane system in terms of dihedral angle, leading to a compound with good affinity at the D_3 receptor and almost 100-fold selectivity over D_2. The tropane system, therefore, demonstrated an initial tractability as lead series and further exploration will be performed in due course.

Table 4. Functional Activity at the Human DA D_3 Receptor and Selectivity for Derivatives **41**−**44**[a]

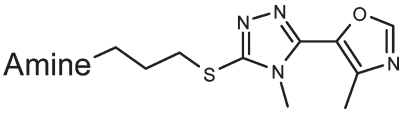

Entry	Amine*	hD_3-GTPγS fpKi	hD_{2L}-GTPγS fpKi	hERG pIC_{50}	cLogD[#]
41	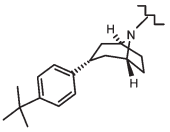	9.2	6.4	6.0	3.7
42	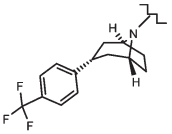	8.0	6.4	6.8	2.6
43	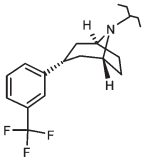	7.3	< 5.5	6.3	2.3
44	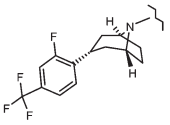	8.2	< 5.5	6.3	2.8

[a] fpK_i = functional pK_i obtained from the GTPγS functional assay. SEM for D_3 GTPγS, and HERG data sets is ±0.1; SEM for the D_{2L} GTPγS data is ±0.2. [#] ACD logD 7.4. Ver 11. * The relative stereochemistry represents the endo isomer.

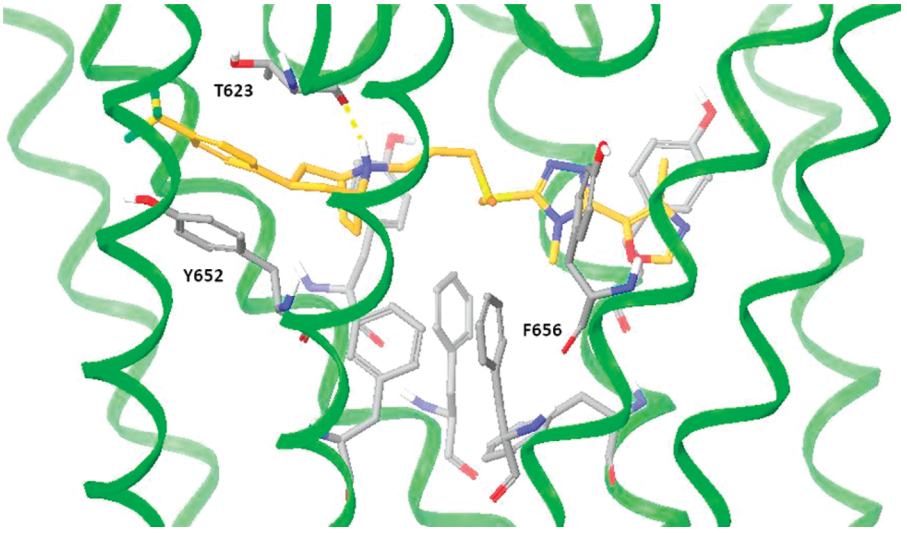

Figure 5. Interactions of compound **42** in the hERG channel models. The backbone ribbon of the pore domain is included but that of the S5 and S6 helices has been removed for clarity. For details about the modeling techniques, please refer to ref 7.

Conclusions

Starting from the potent and selective DA D_3 receptor antagonists previously reported (**1**−**5**), the present work focused on a detailed exploration of the amine moiety of these templates. Rational design and computational tools helped to drive the selection of a number of compounds endowed with high in vitro affinity and selectivity at the DA D_3 receptor. Furthermore, a better understanding of the region of the receptor around Asp 110 was generated through these specific compounds.

Experimental Section

Biological Test Methods. In Vitro Studies. [^{35}S] GTPγS Functional Binding Assay in Cell Membranes Expressing hD_3 Receptors. In vitro functional studies were performed according to the following [^{35}S]-GTPγS protocol. Cells used in the study are Chinese hamster ovary (CHO) cells.

Cell membranes were prepared as follows. Cell pellets were resuspended in 10 volumes of 50 mM HEPES, 1 mM EDTA pH 7.4, using KOH. On the day following, the proteases were added to the buffer just prior to giving the homogenization buffer.

10^{-6} M Leupeptin (Sigma L2884) − 5000 × stock = 5 mg/mL in buffer
25 μg/mL bacitracin (Sigma B0125) − 1000 × stock = 25 mg/mL in buffer
1 mM PMSF − 1000 × stock = 17 mg/mL in 100% ethanol
2×10^{-6} M Pepstain A − 1000 × stock = 2 mM in 100% DMSO

The cells were homogenized by 2 × 15 s bursts in a 1 L glass Waring blender in a class two biohazard cabinet. The resulting suspension was spun at 500*g* for 20 min (Beckman T21 centrifuge: 1550 rpm). The supernatant was withdrawn with a 25 mL pipet, aliquotted into prechilled centrifuge tubes, and spun at 48000*g* to pellet membrane fragments (Beckman T1270: 23000 rpm for 30 min). The final 48000*g* pellet was resuspended in homogenization buffer, (4× the volume of the original cell pellet). The 48000*g* pellet was resuspended by vortexing for 5 s and homogenized in a dounce homogenizer 10−15 stokes. The prep was distributed into appropriate sized aliquots (200−1000 μL) in polypropylene tubes and stored at −800 °C. Protein content in the membrane preparations was evaluated with the Bradford protein assay.

The final top concentration of test drug was 3 μM in the assay, and 11 points serial dilution curves 1:4 in 100% DMSO were carried out using a Biomek FX. The test drug at 1% total assay volume (TAV) was added to a solid, white, 384 well assay plate. fifty percent TAV of precoupled (for 90 min at 4 °C) membranes, 5 μg/well, and wheatgerm agglutinin polystyrene scintillation proximity assay beads (RPNQ0260, Amersham), 0.25 mg/well, in 20 mM HEPES pH 7.4, 100 mM NaCl, 10 mM $MgCl_2$, 60 μg/mL saponin, and 30 μM GDP was added. The third addition was a 20% TAV addition of either buffer, (agonist format) or EC_{80} final assay concentration of agonist, Quinelorane, prepared in assay buffer (antagonist format). The assay was started by the addition of 29% TAV of GTPγ[35S] 0.38 nM final (37 MBq/mL, 1160 Ci/mmol, Amersham). After all additions , assay plates were spun down for 1 min at 1000 rpm. Assay plates were counted on a Viewlux, 613/55 filter, for 5 min, between 2 and 6 h after the final addition.

The effect of the test drug over the basal generates EC_{50} value by an iterative least-squares curve fitting program, expressed in the table as pEC_{50} (i.e., $-\log EC_{50}$). The ratio between the maximal effect of the test drug and the maximal effect of full agonist, Quinelorane, generates the intrinsic activity (IA) value (i.e., IA = 1 full agonist, IA < 1 partial agonist). fpK_i values of test drug were calculated from the IC_{50} generated by "antagonist format" experiment, using Cheng and Prusoff equation: $fK_i = IC_{50}/1 + ([A]/EC50)$ where: [A] is the concentration of the agonist in the assay and EC_{50} is the agonist EC_{50} value obtained in the same experiment. fpK_i is defined as $-\log fK_i$.

hERG-^{3}H Dofetilide Binding Assay. hERG activity was measured using ^{3}H dofetilide binding in a scintillation proximity assay (SPA) format. The activity was measured with a PerkinElmer Viewlux imager.

P450 CYPEX Assay. Inhibition (IC_{50}) of human CYP1A2, 2C9, 2C19, 2D6, and 3A4 was determined using Cypex bactosomes expressing the major human P450s. A range of concentrations (0.1, 0.2, 0.4, 1, 2, 4, and 10 μM) of test compound were prepared in methanol and preincubated at 37 °C for 10 min in 50 mM potassium phosphate buffer (pH 7.4) containing recombinant human CYP450 microsomal protein (0.1 mg/mL; Cypex Limited, Dundee, UK) and probe-fluorescent substrate. The final concentration of solvent was between 3 and 4.5% of the final volume. Following preincubation, NADPH regenerating system (7.8 mg of glucose 6-phosphate, 1.7 mg of NADP, and 6 units of glucose 6-phosphate dehydrogenase/mL of 2% (w/v) $NaHCO_3$; 25 μL) was added to each well to start the reaction. Production of fluorescent metabolite was then measured over a 10 min time course using a Spectrafluor plus plate reader. The rate of metabolite production (AFU/min) was determined at each concentration of compound and converted to a percentage of the mean control rate using Magellan (Tecan software). The inhibition (IC_{50}) of each compound was determined from the slope of the plot using Grafit v5 (Erithacus software, UK). Miconazole was added as a positive control to each plate. CYP450 isoform substrates used were ethoxyresorufin (ER; 1A2; 0.5 μM), 7-methoxy-4-triflouromethylcoumarin-3-acetic acid (FCA; 2C9; 50 μM), 3-butyryl-7-methoxycoumarin (BMC; 2C19; 10 μM), 4-methylaminomethyl-7-methoxycoumarin (MMC; 2D6; 10 μM), diethoxyflourescein (DEF; 3A4; 1 μM), and 7-benzyloxyquinoline (7-BQ; 3A4; 25 μM). The test was performed in three replicates.

Table 5

analytical column	Zorbax SB-C18, 4.6 mm × 50 mm (1.8 μ)
mobile phase	amm acet, 5 mM + 0.1% formic acid/acetonitrile + 0.1% formic acid
gradient	97/3 → 36/64 v/v in 3.5 min → 10/90 in 3.5 min
flow rate	2.0 mL/min
detection	DAD, 210−350 nm
MS	ES+

Intrinsic Clearance (Cli) Assay. Intrinsic clearance (CLi) values were determined in rat and human liver microsomes. Test compounds (0.5 μM) were incubated at 37 °C for 30 min in 50 mM potassium phosphate buffer (pH 7.4) containing 0.5 mg microsomal protein/mL. The reaction was started by addition of cofactor (NADPH; 8 mg/mL). The final concentration of solvent was 1% of the final volume. At 0, 3, 6, 9, 15, and 30 min an aliquot (50 μL) was taken, quenched with acetonitrile containing an appropriate internal standard, and analyzed by HPLC-MS/MS. The intrinsic clearance (CLi) was determined from the first-order elimination constant by nonlinear regression using Grafit v5 (Erithacus software, UK), corrected for the volume of the incubation, and assuming 52.5 mg microsomal protein/g liver for all species. Values for CLi were expressed as mL/min/g liver. The lower limit of quantification of clearance was determined to be when < 15% of the compound had been metabolized by 30 min and this corresponded to a CLi value of 0.5 mL/min/g liver. The upper limit was 50 mL/min/g liver.

Chemical Procedures. General. Experimental. NMR spectra were obtained on Varian INOVA spectrometers (300, 400, and 500 MHz). Chemical shifts are expressed in δ (ppm) units, and peak multiplicity are expressed as follows: singlet (s), doublet (d), doublet of doublets (dd), triplet (t), multiplet (m), broad singlet (br s), broad multiplet (br m). All mass spectrometric measurements were performed using a Micromass Platform LCZ (Waters, Manchester, UK) mass spectrometer operated in positive electrospray ionization mode. When LC/MS detection was performed, analytical conditions were used as reported in Table 5.

General Synthetic Procedures. Appropriate primary or secondary amines (commercially available or prepared in analogy to the procedures described in refs 16−18) were reacted with appropriately decorated 3-[(3-chloropropyl)thio]-4-methyl-4*H*-1,2,4-triazoles (**47**) prepared by the corresponding aryl acids (**45**) in agreement with literature procedures.[7−11] The compounds were suspended/dissolved in dry acetonitrile or DMF reacted in the presence of potassium carbonate according to the reaction Scheme 1 below. Crudes were evaporated and purified by column chromatography. The three compounds reported as single enantiomer (**23**, **25**, **26**) were obtained after preparative chromatography on chiral columns and their enantiomeric purity always verified on analytical column. The enatiomeric excess has been measured by means of SFC analytical techniques. Typical conditions are derived from Chiralpak AD-H column (25 cm × 0.46 cm) with ethanol (+0.1% isopropylamine) 15% as modifier, flow rate 2.5 mL/min, P = 180 bar at 35 °C with detection at 220 nm.

The purity of the compounds reported in the manuscript was established through HPLC-MS methodology. All the compounds reported in the manuscript have a purity >95%.

Scheme 1. General Synthetic Procedures for the Preparation of Compounds **5**−**105**[a]

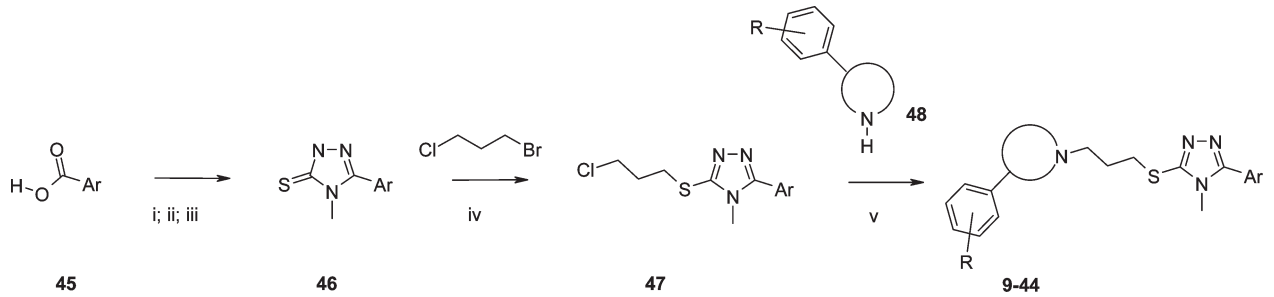

[a] (i) T3P in AcOEt; (ii) 4-methyl-3-thiosemicarbazide; (iii) NaOH; (iv) K_2CO_3/acetone; (v) K_2CO_3/DMF or CH_3CN.

3-(3-{[4-Methyl-5-(4-methyl-1,3-oxazol-5-yl)-4*H*-1,2,4-triazol-3-yl]thio}propyl)-1-phenyl-3-azabicyclo[4.1.0]heptane Hydrochloride (9). ^{1}H NMR (DMSO-d_6): δ 9.93 (bs,1 H), 8.54 (m, 1 H), 7.43 (d, 2 H), 7.31 (m, 2 H), 7.22 (m, 1 H), 3.65 (m, 1 H), 3.38 (m, 8 H), 2.36 (m, 3 H), 2.14 (m, 2 H), 1.49 (m, 5 H). MS (*m*/*z*): 447 $[MH]^+$.

3-(3-{[4-Methyl-5-(4-methyl-1,3-oxazol-5-yl)-4*H*-1,2,4-triazol-3-yl]thio}propyl)-6-phenyl-3-azabicyclo[4.1.0]heptane Hydrochloride (10). ^{1}H NMR (MeOD): δ 8.38 (m, 1 H), 7.44 (d, 2 H), 7.32 (t, 2 H), 4.11 (dd, 1 H), 3.81 (m, 3 H), 3.37 (m, 5 H), 3.15 (dd, 1 H), 2.91 (m, 1 H), 2.57 (m, 1 H), 2.45 (m, 4 H), 2.27 (m, 2 H), 1.66 (m, 1 H), 1.29 (m, 1 H), 1.17 (m, 1 H). MS (*m*/*z*): 447 $[MH]^+$.

3-(3-{[4-Methyl-5-(4-methyl-1,3-oxazol-5-yl)-4*H*-1,2,4-triazol-3-yl]thio}propyl)-1-[4-(trifluoromethyl)phenyl]-3-azabicyclo-[4.1.0]heptane Hydrochloride (11). ^{1}H NMR (DMSO-d_6): δ 9.97 (bs,1 H), 8.57 (m, 1 H), 7.65 (m, 4 H), 3.89 (m, 1 H), 3.68 (m, 3 H), 3.24 (m, 6 H), 2.85 (m, 1 H), 2.54 (m, 1 H), 2.38 (s, 3 H), 2.19 (m, 2 H), 2.07 (m, 1 H), 1.38 (m, 3 H). MS (*m*/*z*): 478 $[MH]^+$.

3-(3-{[4-Methyl-5-(4-methyl-1,3-oxazol-5-yl)-4*H*-1,2,4-triazol-3-yl]thio}propyl)-6-[4-(trifluoromethyl)phenyl]-3-azabicyclo-[4.1.0]heptane Hydrochloride (12). ^{13}C NMR (DMSO-d_6): δ 152.1, 150.7, 149.9, 146.2, 137.2, 134.3, 128.9, 127.8, 127.1 (q, J = 30.9 Hz), 125.3, 125.1 (q, J = 3.9 Hz), 124.3 (q, J = 271.6 Hz), 54.0, 50.2, 46.4, 31.7, 30.0, 27.2, 23.4, 22.8, 16.8, 15.3, 12.3.

3-(3-{[4-Methyl-5-(4-methyl-1,3-oxazol-5-yl)-4*H*-1,2,4-triazol-3-yl]thio}propyl)-6-[3-(trifluoromethyl)phenyl]-3-azabicyclo-[4.1.0]heptane Hydrochloride (14). ^{13}C NMR (DMSO-d_6): δ 152.1, 150.7, 146.6, 146.2, 137.1, 134.4, 132.5, 129.3, 129.1 (q, J = 31.9 Hz), 124.9, 124.1 (q, J = 272.6 Hz), 123.2, 54.0, 50.3, 46.4, 31.7, 30.0, 27.7, 23.4, 22.9, 16.4, 15.1, 12.3.

4-(3-{[5-(2,4-Dimethyl-1,3-oxazol-5-yl)-4-methyl-4*H*-1,2,4-triazol-3-yl]thio}propyl)-1-[4-(trifluoromethyl)phenyl]-4-azabicyclo-[5.1.0]octane Hydrochloride (16). ^{13}C NMR (DMSO-d_6): δ 161.4, 150.6, 149.6, 146.2, 138.1, 133.7, 128.4, 126.6 (q, J = 30.9 Hz), 125.2 (q, J = 3.9 Hz), 124.4 (q, J = 271.6 Hz), 55.7, 55.6, 53.3, 31.8, 31.0, 30.2, 27.2, 26.9, 25.8, 23.8, 23.2, 13.6, 12.3.

4-(3-{[5-(2,4-Dimethyl-1,3-thiazol-5-yl)-4-methyl-4*H*-1,2,4-triazol-3-yl]thio}propyl)-1-[4-(trifluoromethyl)phenyl]-4-azabicyclo[5.1.0]-octane Hydrochloride (17). ^{13}C NMR (DMSO-d_6): δ 167.6, 153.6, 151.1, 149.5, 148.1, 128.3, 126.6 (q, J = 31.9 Hz), 125.2, 125.1 (q, J = 3.9 Hz), 124.0 (q, J = 271.8 Hz), 55.7, 55.6, 53.3, 31.6, 30.9, 30.0, 27.1, 26.9, 25.8, 23.9, 23.2, 18.8, 16.1.

4-(3-{[4-Methyl-5-(4-pyridazinyl)-4*H*-1,2,4-triazol-3-yl]thio}-propyl)-1-[4-(trifluoromethyl)phenyl]-4-azabicyclo[5.1.0]octane (18). ^{1}H NMR (DMSO-d_6): δ 9.65 (d, 1 H), 9.4 (d, 1 H), 7.90 (d, 1 H), 7.70 (d, 2 H), 7.42 (d, 2 H), 3.75 (s, 3 H), 3.45 (t, 2 H), 2.96 (m, 1 H), 2.77 (m, 1 H), 2.65 (t, 2 H), 2.54 (m, 2 H), 2.35 (m, 2 H), 2.19 (m, 2 H), 1.8 (m, 1 H), 1.65 (s, 3 H), 1.40 (m,1 H), 1.09 (d, 1 H), 0.95 (m, 1 H). MS (*m*/*z*): 489.2 $[MH]^+$.

^{13}C NMR (DMSO-d_6): δ 152.6, 151.8, 151.1, 149.5, 149.1, 128.3, 126.6 (q, J = 31.9 Hz), 125.7, 125.2 (q, J = 3.9 Hz), 124.5 (q, J = 271.6 Hz), 55.8, 55.6, 53.3, 32.1, 31.0, 29.9, 27.1, 27.0, 25.8, 24.0, 23.2.

(3-{[4-Methyl-5-(4-methyl-1,3-oxazol-5-yl)-4*H*-1,2,4-triazol-3-yl]-thio}propyl)-1-phenylbicyclo[3.1.0]hexan-3-amine Hydrochloride (21). ^{1}H NMR (DMSO-d_6): δ 8.60−8.51 (m, 1 H), 7.31−7.22 (m, 2 H), 7.20−7.10 (m, 3 H), 4.07−3.87 (m, 1 H), 3.71−3.63 (s, 3 H), 3.32−3.20 (t, 2 H), 3.09−2.90 (m, 2 H), 2.74−2.61 (m, 1 H), 2.61−2.50 (m, 1 H), 2.39−2.32 (s, 3 H), 2.15−2.07 (m, 1 H), 2.10−1.94 (m, 2 H), 1.83−1.62 (m, 2 H), 1.27−1.18 (m, 1 H), 1.10−1.01 (m, 1 H).

(3-{[4-Methyl-5-(4-methyl-1,3-oxazol-5-yl)-4*H*-1,2,4-triazol-3-yl]-thio}propyl){(1*S*,2*R*,5*S*)-5-[4-(trifluoromethyl)phenyl]bicyclo-[3.1.0]hex-2-yl}amine Hydrochloride (23). ^{13}C NMR (DMSO-d_6): δ 152.0, 151.2, 150.2, 146.0, 137.0, 134.4, 126.1, 125.7 (q, J = 31.9 Hz), 124.9 (q, J = 3.9 Hz), 124.6 (q, J = 271.6 Hz), 59.2, 46.3, 31.5, 30.9, 30.7, 30.6, 29.7, 28.9, 27.3, 15.4, 12.2.

{5-[2-Fluoro-4-(trifluoromethyl)phenyl]bicyclo[3.1.0]hex-2-yl}-(3-{[4-methyl-5-(4-methyl-1,3-oxazol-5-yl)-4*H*-1,2,4-triazol-3-yl]-thio}propyl)amine Hydrochloride (25). ^{13}C NMR (DMSO-d_6): δ 161.2 (d, J = 247.4 Hz), 152.1, 150.8, 146.2, 137.1, 134.5 (d, J = 13.5 Hz), 134.3, 131.8 (d, J = 3.9 Hz), 129.1, 123.4 (q, J = 274.5 Hz), 121.3, 112.9 (dq, J = 25.1 Hz, 3.9 Hz), 59.1, 44.5, 31.7, 30.8, 29.8, 28.6, 25.9, 24.0, 23.8, 12.2, 12.0.

5-[2-Fluoro-4-(trifluoromethyl)phenyl]bicyclo[3.1.0]hex-2-yl}-(3-{[4-methyl-5-(4-methyl-1,3-oxazol-5-yl)-4*H*-1,2,4-triazol-3-yl]-thio}propyl)amine Hydrochloride (26). ^{13}C NMR (DMSO-d_6): δ 161.2 (d, J = 247.4 Hz), 152.1, 150.8, 146.2, 137.1, 134.5 (d, J = 13.5 Hz), 134.3, 131.8 (d, J = 3.9 Hz), 129.1, 123.4 (q, J = 274.5 Hz), 121.3, 112.9 (dq, J = 25.1 Hz, 3.9 Hz), 59.1, 44.5, 31.7, 30.8, 29.8, 28.6, 25.9, 24.0, 23.8, 12.2, 12.0.

6-Bromo-1′-(3-{[4-methyl-5-(4-methyl-1,3-oxazol-5-yl)-4*H*-1,2,4-triazol-3-yl]thio}propyl)-3,4-dihydro-2*H*-spiro[naphthalene-1,3′-pyrrolidine] Hydrochloride (28). ^{1}H NMR (DMSO-d_6) δ ppm 10.44 (br s, 1 H), 8.55−8.58 (m, 1 H), 7.56 (d, 1 H), 7.34−7.43 (m, 1 H), 7.29−7.32 (m, 1 H), 3.70−3.82 (m, 2 H), 3.65−3.71 (m, 3 H), 3.22−3.48 (m, 5 H), 3.10−3.21 (m, 1 H), 2.67−2.76 (m, 2 H), 2.32−2.41 (m, 4 H), 1.78−2.27 (m, 7 H), 1.64−1.76 (m, 2 H).

7-Bromo-1′-(3-{[4-methyl-5-(4-methyl-1,3-oxazol-5-yl)-4*H*-1,2,4-triazol-3-yl]thio}propyl)-3,4-dihydro-2*H*-spiro[naphthalene-1,3′-pyrrolidine] Hydrochloride (29). ^{1}H NMR (DMSO-d_6) δ ppm 10.48 (br s, 1 H), 8.55−8.58 (m, 1 H), 7.80−7.89 (m, 1 H), 7.28−7.36 (m, 1 H), 7.00−7.08 (m, 1 H), 3.70−3.87 (m, 2 H), 3.67−3.70 (m, 3 H), 3.34−3.41 (m, 2 H), 3.25−3.32 (m, 2 H), 3.11−3.26 (m, 2 H), 2.67−2.68 (m, 2 H), 2.35−2.38 (m, 3 H), 2.34−2.44 (m, 1 H), 2.02−2.29 (m, 3 H), 1.63−2.03 (m, 4 H).

1′-(3-{[4-Methyl-5-(4-methyl-1,3-oxazol-5-yl)-4*H*-1,2,4-triazol-3-yl]thio}propyl)-6-(methyloxy)-3,4-dihydro-2*H*-spiro[naphthalene-1,3′-pyrrolidine] Hydrochloride (30). ^{1}H NMR (DMSO-d_6) δ ppm 10.34 (br s, 1 H), 8.49−8.60 (m, 1 H), 7.48 (d, 1 H), 6.72−6.84 (m, 1 H), 6.54−6.65 (m, 1 H), 3.63−3.79 (m, 8 H), 3.05−3.50 (m, 6 H), 2.61−2.77 (m, 2 H), 2.32−2.40 (m, 3 H), 2.25−2.44 (m, 1 H), 2.08−2.22 (m, 2 H), 1.55−2.07 (m, 5 H).

1′-(3-{[4-Methyl-5-(4-methyl-1,3-oxazol-5-yl)-4*H*-1,2,4-triazol-3-yl]thio}propyl)-5-(methyloxy)-3,4-dihydro-2*H*-spiro[naphthalene-1,3′-pyrrolidine] Hydrochloride (31). ^{1}H NMR (DMSO-d_6) δ ppm 10.54 (br s, 1 H), 8.52−8.61 (m, 1 H), 7.11−7.29 (m, 2 H), 6.75−6.85 (m, 1 H), 3.74−3.75 (m, 3 H), 3.71−3.81 (m, 2 H), 3.66−3.70 (m, 3 H), 3.34−3.49 (m, 3 H), 3.24−3.32 (m, 2 H), 3.11−3.22 (m, 1 H), 2.56−2.65 (m, 1 H), 2.43−2.54 (m, 1 H), 2.35−2.37 (m, 3 H), 2.32−2.41 (m, 1 H), 2.09−2.25 (m, 2 H), 1.92−2.09 (m, 1 H), 1.60−1.92 (m, 4 H).

1′-(3-{[4-Methyl-5-(4-methyl-1,3-oxazol-5-yl)-4*H*-1,2,4-triazol-3-yl]thio}propyl)-7-(methyloxy)-3,4-dihydro-2*H*-spiro[naphthalene-1,3′-pyrrolidine] Hydrochloride (32). ^{1}H NMR (DMSO-d_6) δ ppm 10.12−11.03 (m, 1 H), 8.50−8.62 (m, 1 H), 7.04−7.28 (m, 1 H), 6.91−7.04 (m, 1 H), 6.66−6.82 (m, 1 H), 3.73−3.76 (m, 3 H), 3.69−3.87 (m, 2 H), 3.66−3.70 (m, 3 H), 3.23−3.51 (m, 5 H), 3.10−3.24 (m, 1 H), 2.59−2.68 (m, 2 H), 2.36−2.47 (m, 1 H), 2.34−2.37 (m, 3 H), 1.62−2.23 (m, 7 H).

1′-(3-{[4-Methyl-5-(4-methyl-1,3-oxazol-5-yl)-4*H*-1,2,4-triazol-3-yl]thio}propyl)-2,3-dihydrospiro[chromene-4,3′-pyrrolidine] Hydrochloride (33). ^{1}H NMR (DMSO-d_6) δ ppm 10.60 (br s, 1 H), 8.54−8.59 (m, 1 H), 7.53−7.61 (m, 1 H), 7.09−7.17 (m, 1 H), 6.91−6.97 (m, 1 H), 6.73−6.79 (m, 1 H), 4.07−4.21 (m, 2 H), 3.73−3.85 (m, 2 H), 3.66−3.70 (m, 3 H), 3.26−3.31 (m, 2 H), 3.22−3.50 (m, 4 H), 2.39−2.47 (m, 1 H), 2.35−2.38 (m, 3 H), 1.93−2.28 (m, 5 H).
^{13}C NMR (DMSO-d_6): δ 153.5, 152.0, 151.3, 146.0, 137.0, 134.4, 130.9, 127.8, 126.9, 120.6, 116.1, 69.0, 63.6, 53.7, 53.6, 41.7, 40.6, 35.6, 31.5, 30.9, 28.1, 12.2.

5-Bromo-1′-(3-{[3-(4-methyl-1,3-oxazol-5-yl)-1*H*-1,2,4-triazol-5-yl]thio}propyl)-2,3-dihydrospiro[indene-1,3′-pyrrolidine] Hydrochloride (34). ^{1}H NMR (DMSO-d_6) δ ppm 1.82−2.39 (m, 6 H), 2.29−2.35 (m, 3 H), 2.76−2.92 (m, 2 H), 3.04−3.49 (m, 6 H), 3.57−3.80 (m, 2 H), 3.64 (s, 3 H), 7.30−7.50 (m, 3 H), 8.44−8.58 (m, 1 H), 10.70 (br s, 1 H).

4-Bromo-1′-(3-{[4-methyl-5-(4-methyl-1,3-oxazol-5-yl)-4*H*-1,2,4-triazol-3-yl]thio}propyl)-2,3-dihydrospiro[indene-1,3′-pyrrolidine] Hydrochloride (35). ^{13}C NMR (DMSO-d_6): δ 152.9, 152.0, 151.3, 146.0, 142.9, 137.0, 134.4, 129.2, 129.0, 121.9, 118.9, 66.5, 54.7, 53.7, 53.6, 39.4, 39.0, 31.6, 31.5, 30.8, 28.2, 12.3.

6-Bromo-1′-(3-{[4-methyl-5-(4-methyl-1,3-oxazol-5-yl)-4*H*-1,2,4-triazol-3-yl]thio}propyl)-2,3-dihydrospiro[indene-1,3′-pyrrolidine] Hydrochloride (36). ^{13}C NMR (DMSO-d_6): δ 153.6, 152.0, 151.3, 146.1, 142.2, 137.0, 134.4, 129.1, 126.2, 125.6, 119.3, 66.2, 53.7, 53.5, 53.4, 40.4, 38.5, 31.5, 30.9, 29.7, 28.2, 12.3.

6-Chloro-1′-(3-{[5-(2,4-dimethyl-1,3-thiazol-5-yl)-4-methyl-4*H*-1,2,4-triazol-3-yl]thio}propyl)-2,3-dihydrospiro[indene-1,3′-pyrrolidine] Hydrochloride (37). ^{13}C NMR (DMSO-d_6): δ 166.8, 153.2, 153.1, 151.2, 148.2, 141.7, 130.9, 126.3, 125.7, 122.6, 114.8, 66.2, 53.7, 53.5, 53.4, 40.5, 38.5, 31.2, 30.7, 29.6, 28.2, 18.8, 16.1.

5-Chloro-1′-(3-{[5-(2,4-dimethyl-1,3-thiazol-5-yl)-4-methyl-4*H*-1,2,4-triazol-3-yl]thio}propyl)-2,3-dihydrospiro[indene-1,3′-pyrrolidine] Hydrochloride (38). ^{13}C NMR (DMSO-d_6): δ 166.8, 153.2, 151.1, 148.2, 145.4, 143.9, 133.9, 126.5, 124.3, 124.1, 114.8, 62.8, 53.7, 53.6, 52.9, 40.3, 38.4, 31.2, 30.5, 30.0, 27.8, 18.8, 16.1.

1′-(3-{[5-(2,4-Dimethyl-1,3-thiazol-5-yl)-4-methyl-4*H*-1,2,4-triazol-3-yl]thio}propyl)-5-fluoro-2,3-dihydrospiro[indene-1,3′-pyrrolidine] Hydrochloride (39). ^{13}C NMR (DMSO-d_6): δ 166.8, 161.4 (d, J = 239.7 Hz), 153.2, 151.2, 148.2, 146.4, 145.3 (d, J = 8.7 Hz), 123.8 (d, J = 8.7 Hz), 114.8, 113.2 (d, J = 22.2 Hz), 110.9 (d, J = 21.3 Hz), 66.4, 53.8, 53.6, 52.6, 40.9, 38.8, 31.2, 30.7, 30.1, 28.3, 18.8, 16.1.

1′-(3-{[5-(2,4-Dimethyl-1,3-thiazol-5-yl)-4-methyl-4*H*-1,2,4-triazol-3-yl]thio}propyl)-6-fluoro-2,3-dihydrospiro[indene-1,3′-pyrrolidine] Hydrochloride (40). ^{13}C NMR (DMSO-d_6): δ 166.8, 161.7 (d, J = 240.7 Hz), 153.2, 153.1 (d, J = 7.7 Hz), 151.2, 148.2, 138.4, 125.3 (d, J = 8.7 Hz), 114.8, 113.1 (d, J = 22.2 Hz), 109.5 (d, J = 22.2 Hz), 66.1, 53.8, 53.6, 53.5, 40.9, 38.5, 31.2, 30.7, 29.4, 28.2, 18.8, 16.1.

3-[4-(1,1-Dimethylethyl)phenyl]-8-(3-{[4-methyl-5-(4-methyl-1,3-oxazol-5-yl)-4*H*-1,2,4-triazol-3-yl]thio}propyl)-8-azabicyclo-[3.2.1]octane Hydrochloride (41). ^{1}H NMR (MeOD): δ ppm 8.43 (s, 1 H) 7.42 (d, 2 H) 7.37 (d, 2 H) 4.04 (m, 2 H) 3.77 (s, 3 H) 3,23 (t, 2 H) 3,3 (br. s, 1 H) 3.18 (t, 2 H) 2.62 (m, 4 H) 2.42 (s, 3 H), 2.24 (m, 2 H), 2.10 (m, 2 H), 1.83 (m, 2 H), 1.27 (s, 9 H).
^{13}C NMR (DMSO-d_6): δ 152.1, 150.9, 148.1, 146.2, 139.8, 137.2, 134.3, 126.1, 124.9, 60.6, 49.2, 34.0, 32.3, 31.7, 31.1, 29.6, 29.2, 24.4, 23.6, 12.3.

8-(3-{[4-Methyl-5-(4-methyl-1,3-oxazol-5-yl)-4*H*-1,2,4-triazol-3-yl]thio}propyl)-3-[4-(trifluoromethyl)phenyl]-8-azabicyclo[3.2.1]-octane (42). ^{13}C NMR (DMSO-d_6): δ 152.0, 151.4, 151.2, 146.0, 137.0, 134.4, 128.0, 126.3 (q, J = 31.9 Hz), 124.8 (q, J = 3.9 Hz), 124.3 (q, J = 271.6 Hz), 57.1, 50.1, 38.2, 32.6, 31.6, 30.9, 28.6, 28.3, 12.2.

8-(3-{[4-Methyl-5-(4-methyl-1,3-oxazol-5-yl)-4*H*-1,2,4-triazol-3-yl]thio}propyl)-3-[3-(trifluoromethyl)phenyl]-8-azabicyclo[3.2.1]-octane (43). ^{13}C NMR (DMSO-d_6): δ 152.0, 151.4, 147.7, 146.0, 137.0, 134.4, 131.5, 129.0, 128.8 (q, J = 31.9 Hz), 124.4 (q, J = 272.6 Hz), 123.6 (q, J = 3.9 Hz), 122.3 (q, J = 3.9 Hz), 57.0, 50.2, 38.6, 32.5, 31.5, 30.9, 28.7, 28.5, 12.2.

3-[2-Fluoro-4-(trifluoromethyl)phenyl]-8-(3-{[4-methyl-5-(4-methyl-1,3-oxazol-5-yl)-4*H*-1,2,4-triazol-3-yl]thio}propyl)-8-azabicyclo[3.2.1]-octane (44). ^{13}C NMR (DMSO-d_6): δ 160.1 (d, J = 246.5 Hz), 152.0, 151.4, 146.0, 137.9 (d, J = 13.5 Hz), 137.0, 134.4, 130.2 (d, J = 4.9 Hz), 128.2 (dq, J = 32.9 Hz, 8.7 Hz), 123.4 (q, J = 271.6 Hz), 121.2, 112.5 (dq, J = 27.1 Hz, 3.9 Hz), 56.7, 50.3, 37.9, 31.5, 31.0, 29.1, 28.7, 26.4, 12.2.

Acknowledgment. We thank Dr. Stefano Fontana, Dr. Chiara Savoia, Dr. Francesca Cardullo, Dr. Elettra Fazzolari, and Silvia Tomelleri for the management of some of the compounds reported in this manuscript. We also thank Dr. Daniele Donati, Dr. Tino Rossi, and Dr. Jim Hagan for the fruitful discussions during the life of the programme.

Supporting Information Available: Computational chemistry details and additional pharmacophore fitting with the new model. This material is available free of charge via the Internet at http://pubs.acs.org.

References

(1) Heidbreder, C. A.; Newman, A. H. Current perspectives on selective dopamine D_3 receptor antagonists as pharmacotherapeutics for addictions and related disorders. *Ann. N.Y. Acad. Sci.* **2010**, *1187*, 4–34.
(2) Joyce, J. N.; Millan, M. J. DA D_3 receptor antagonists as therapeutic agents. *Drug Discovery Today* **2005**, *10*, 917–925.
(3) Micheli, F.; Heidbreder, C. Selective DA D_3 receptor antagonists: A review 2001−2005. *Recent Pat. CNS Drug Discovery* **2006**, *1*, 271–288.
(4) Newman, A. H.; Grundt, P.; Nader, M. A. DA D_3 receptor partial agonists and antagonists as potential drug abuse therapeutic agents. *J. Med. Chem.* **2005**, *48*, 3663–3679.
(5) Micheli, F.; Heidbreder, C. A. Selective Dopamine D_3 Receptor Antagonists; 1997−2007: A Decade of Progress. *Expert Opin. Ther. Pat.* **2008**, *18*, 821–840.
(6) Heidbreder, C. Selective antagonism at dopamine D_3 receptors as a target for drug addiction pharmacotherapy: a review of preclinical evidence. *CNS Neurol. Disord. Drug Targets* **2008**, *7*, 410–421.
(7) Micheli, F.; Arista, L.; Bonanomi, G.; Blaney, F. E.; Braggio, S.; Capelli, A. M.; Checchia, A.; Damiani, F.; Di Fabio, R.; Fontana, S.; Gentile, G.; Griffante, C.; Hamprecht, D.; Marchioro, C.; Mugnaini, M.; Piner, J.; Ratti, E.; Tedesco, G.; Tarsi, L.; Terreni, S.; Worby, A.; Ashby, C. R., Jr.; Heidbreder, C. 1,2,4-Triazolyl azabicyclo[3.1.0]hexanes: a new series of potent and selective dopamine D_3 receptor antagonists. *J. Med. Chem.* **2010**, *53*, 374–391.
(8) Bonanomi, G.; Braggio, S.; Capelli, A. M.; Checchia, A.; Di Fabio, R.; Marchioro, C.; Tarsi, L.; Tedesco, G.; Terreni, S.; Worby, a.; Heidbreder, C.; Micheli, F. Triazolyl Azabicyclo[3.1.0]hexanes: A Class of Potent and Selective Dopamine D_3 Receptor Antagonists. *ChemMedChem* **2010**, *5*, 705–715.
(9) Micheli, F.; Bonanomi, G.; Blaney, F. E.; Braggio, S.; Capelli, A. M.; Checchia, A.; Curcuruto, O.; Damiani, F.; Di-Fabio, R.; Donati, D.; Gentile, G.; Gribble, A.; Hamprecht, D.; Tedesco, G.; Terreni, S.; Tarsi, L.; Lightfoot, A.; Pecoraro, M.; Petrone, M.; Perini, O.; Piner, J.; Rossi, T.; Worby, A.; Pilla, M.; Valerio, E.; Griffante, C.; Mugnaini, M.; Wood, M.; Scott, C.; Andreoli, M.; Lacroix, L.; Schwarz, A.; Gozzi, A.; Bifone, A.; Ashby, C. R., Jr.; Hagan, J. J.; Heidbreder, C. 1,2,4-Triazol-3-yl-thiopropyl-tetrahydrobenzazepines: a series of potent and selective dopamine D_3 receptor antagonists. *J. Med. Chem.* **2007**, *50*, 5076–5089.
(10) Micheli, F.; Bonanomi, G.; Braggio, S.; Capelli, A. M.; Celestini, P.; Damiani, F.; Di Fabio, R.; Donati, D.; Gagliardi, S.; Gentile, G.; Hamprecht, D.; Petrone, M.; Radaelli, S.; Tedesco, G.; Terreni, S.; Worby, A.; Heidbreder, C. New fused benzazepine as selective

D_3 receptor antagonists. Synthesis and biological evaluation. Part one: [h]-fused tricyclic systems. *Bioorg. Med. Chem. Lett.* **2008**, *18*, 901–907.
(11) Micheli, F.; Bonanomi, G.; Braggio, S.; Capelli, A. M.; Celestini, P.; Damiani, F.; Di Fabio, R.; Donati, D.; Gagliardi, S.; Gentile, G.; Hamprecht, D.; Perini, O.; Petrone, M.; Radaelli, S.; Tedesco, G.; Terreni, S.; Worby, A.; Heidbreder, C. New fused benzazepine as selective D_3 receptor antagonists. Synthesis and biological evaluation. Part two: [g]-fused and hetero fused systems. *Bioorg. Med. Chem. Lett.* **2008**, *18*, 908–912.
(12) Reavill, C.; Taylor, S. G.; Wood, M. D.; Ashmeade, T.; Austin, N. E.; Avenell, K. Y.; Boyfield, I.; Branch, C. L.; Cilia, J.; Coldwell, M. C.; Hadley, M. S.; Hunter, A. J.; Jeffrey, P.; Jewitt, F.; Johnson, C. N.; Jones, D. N.; Medhurst, A. D.; Middlemiss, D. N.; Nash, D. J.; Riley, G. J.; Routledge, C.; Stemp, G.; Thewlis, K. M.; Trail, B.; Vong, A. K.; Hagan, J. J. Pharmacological actions of a novel, high-affinity, and selective human dopamine D_3 receptor antagonist, SB-277011-A. *J. Pharmacol. Exp. Ther.* **2000**, *294*, 1154–65.
(13) Macdonald, G. J.; Branch, C. L.; Hadley, M. S.; Johnson, C. N.; Nash, D. J.; Smith, A. B.; Stemp, G.; Thewlis, K. M.; Vong, A. K.; Austin, N. E.; Jeffrey, P.; Winborn, K. Y.; Boyfield, I.; Hagan, J. J.; Middlemiss, D. N.; Reavill, C.; Riley, G. J.; Watson, J. M.; Wood, M.; Parker, S. G.; Ashby, C. R., Jr. Design and synthesis of *trans*-3-(2-(4-((3-(3-(5-methyl-1,2,4-oxadiazolyl))- phenyl)carboxamido)-cyclohexyl)ethyl)-7-methylsulfonyl-2,3,4,5-tetrahydro-1*H*-3-benzazepine (SB-414796): a potent and selective dopamine D_3 receptor antagonist. *J. Med. Chem.* **2003**, *46*, 4952–4964.
(14) *Catalyst 4.11*; Accelrys Inc.
(15) Ballesteros, J. A.; Weinstein, H. Integrated methods for the construction of three-dimensional models and computational probing of structure-function relationships in G-protein coupled receptors. *Methods Neurosci.* **1995**, *25*, 366–428.
(16) Skolnick, P.; Chen, Z.; Yang, Ji. Arylbicyclo[3.1.0]hexylamines as inhibitors against monoamine neurotransmitter transports and their preparation, pharmaceutical compositions and use in the treatment of CNS disorders. PCT Int. Appl. WO2008057575, 2008.
(17) Bertani, B.; Di Fabio, R.; Micheli, F.; Pasquarello, A.; Tarsi, L.; Terreni, S. Spiro compounds, processes for preparing them, pharmaceutical compositions containing them, and their use as as modulators of dopamine D_3 receptors. PCT Int. Appl. WO2007125061, 2007.
(18) (a) Di Fabio, R.; Micheli, F.; Tedesco, G.; Terreni, S. Preparation of 3-azabicyclo[4.1.0]heptanes as therapeutic monoamine reuptake inhibitors. PCT Int. Appl. WO2008031771, 2008; (b) Bertani, B.; Di Fabio, R.; Micheli, F.; Tedesco, G.; Terreni, S. Preparation of azabicyclic compounds as inhibitors of mono-amines re-uptake and antidepressant agents. PCT Int. Appl. WO2008031772, 2008.